Superradiant Forward Scattering in Multiple Scattering

Julien Chabé[1], Louis Bellando,[1] Tom Bienaimé,[1] Romain Bachelard,[2] Nicola Piovella,[3] and Robin Kaiser[1]

[1] *Université de Nice Sophia Antipolis, CNRS, Institut Non-Linéaire de Nice, UMR 7335, F-06560 Valbonne, France*
[2] *Instituto de Física de São Carlos, Universidade de São Paulo, 13560-970 São Carlos, SP, Brazil*
[3] *Dipartimento di Fisica, Università Degli Studi di Milano, Via Celoria 16, I-20133 Milano, Italy*

(Dated: October 29, 2012)

We report on an interference effect in multiple scattering by resonant scatterers resulting in enhanced forward scattering, violating Ohm's law for photons. The underlying mechanism of this wave effect is superradiance, which we have investigated using cold atoms as a toy model. We present numerical and experimental evidences for this superradiant forward scattering, which is robust against disorder and configuration averaging.

PACS numbers: 42.50.Gy, 42.25.Bs, 03.65.Yz , 32.80.Qk

A rigorous investigation of light propagation in the presence of many scatterers requires taking into account the effects of interferences. Fortunately in most situations interference effects can be neglected and a radiative transfer equation is thus often used in optics, allowing a practical approach to scattering of light in complex media. Some exceptions are however known, where interferences are fundamental for the observed features. One prominent feature is coherent backscattering (CBS) [1, 2]. Interferences also come into play in experiments on universal conductance fluctuations [3] and more recent experiments probing the local density of states [4–6]. A very active line of research concerns strong localization of waves of light [7, 8]. However, beyond these examples few features where interference effects survive after configuration average in optical dense media are known. In the limit of very dense samples, close to the strong localization regime, another hitherto non observed features is coherent forward scattering [9]. Most of the above features are genuine wave effects and can be present in the propagation of different types of waves, such as matter waves [10–13] or acoustics [14, 15].

If scattering of light is enhanced by a narrow resonance, additional features appear. Indeed at resonance the polarisability becomes imaginary, describing the opening of the system to many vacuum modes. As a result cooperative scattering as pioneered by Dicke [16] leads to superradiance [17–19, 23, 24] investigated in various recent experiments [20–22]. Analytical investigations are difficult, as a rigorous theory for wave propagation in multiple scattering is not developed. In order to go beyond numerical studies, one either resorts to an effective index approach [25] or a diagrammatic analysis [26]. For resonant scattering, these approaches are however not valid [27] and the situation is reminiscent of resonant scattering by matter waves at the unitary limit [28, 29].

In this letter we present a new interference effect in multiple scattering. We start our investigation of this steady state superradiant forward scattering (SFS) in the multiple scattering regime using numerical simulations before presenting experimental results of such phenomenon.

The relevance of interference effects in multiple scattering is best highlighted by a comparison to an incoherent model, where the propagation of photons are described by classical ray optics. We investigate the role of interferences using different wave models. The first one is a microscopic model based on N coupled dipole equations [30], a type of many body solution for our wave equation. We also use two analytical models which amount to a rough mean field Ansatz: the driven timed Dicke model [18, 31], where the N randomly-distributed particles have the same amplitude and a phase imprinted by the laser, successfully used to describe previous experiments and a partial wave approach [32] used to predict Mie resonances. We choose to use a simplified scalar model (instead of the more rigorous vectorial model [17]) as this highlights the essence of SFS which does not rely on the specific vectorial nature of light.

A textbook situation to study the propagation of light through disordered media is the slab configuration. We focus our interest in this letter on resonant scattering and define the optical thickness $b_0 = n\sigma_0 L$, where n is the spatial density of atoms, $\sigma_0 = 3\lambda^2/2\pi$ the resonant cross section at the wavelength λ for individual two-level atoms and kL the thickness of the slab in units of $k^{-1} = \lambda/2\pi$. In the absence of cooperative effects, this optical thickness is related to the forward (ballistic) transmission via $T_{\rm coh} = e^{-b_0}$. We compute the intensity distribution inside the slab and the diffuse transmission through the sample using different numerical methods. As one can see in Fig. 1, the intensity distribution obtained from our many body solution (blue squares in Fig. 1) inside the sample for an optical thickness of $b_0 = 8$ is far from being uniform. This might *a priori* not come as a surprise, as an incoherent model of multiple scattering of photons undergoing a random walk inside the sample provides a similar intensity distribution (black circles in Fig. 1). For this incoherent model we perform a Monte Carlo simulation, isotropically scattering photons after a scattering mean free path $l_{\rm sc} = L/b_0$, where L is the thickness of the slab. We note that for the many body

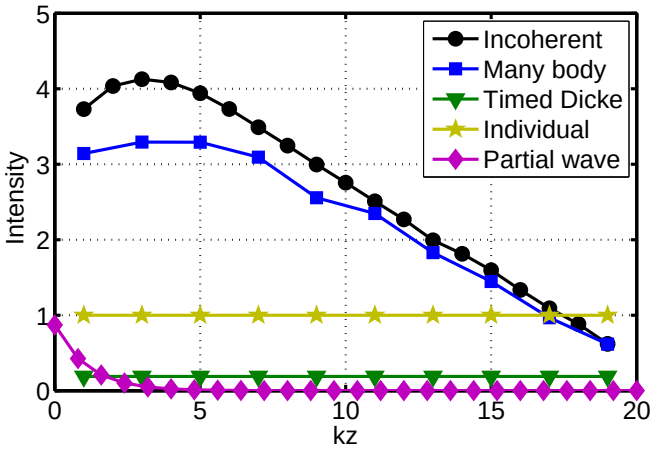

FIG. 1: (color online). Intensity distribution inside a slab with thickness of atoms with a thickness $L_z = 20/k$ and $b_0 = 8$ and a transverse size of $L_x = L_y = 80/k$. The local intensity inside the slab is computed using an incoherent model (black spheres) and compared to the excited state population derived in a driven timed Dicke model (green triangles) and a partial wave Ansatz (pink diamonds). The limit of independent dipoles (yellow stars) is recovered in the driven timed Dicke model for $b_0 \to 0$. The many body solution is obtained using N coupled dipole equations (blue squares).

solution, the local field has important fluctuations reflecting the speckle nature of the field in multiple scattering. For the data shown in Fig. 1 we have thus used an integration over the transverse directions inside the slab, applied a coarse graining with a resolution of $k\delta z = 2$ and averaged over 30 configurations. As one can see in Fig. 1 our driven timed Dicke model very poorly describes the intensity distribution inside the sample: for the slab geometry considered here, the population of the excited state (green triangles in Fig. 1), homogeneous in this Ansatz, scales as $(1 + b_0/6)^{-2}$[33]. When using a dilute sample (vanishing b_0) this model recovers the independent atom case (yellow stars in Fig. 1). For large b_0 however only the first layer of the sample is excited by the incident field alone. Dipoles located in the deeper layers of the sample are excited by the interference of the incident field with the field scattered by all other dipoles and the homogeneous Ansatz for dipole excitation is no longer appropriate. We also show the result of a partial wave approach (pink diamonds in Fig. 1), expected to be valid not only when the dipole are excited by the external field. However this model assumes an effective index response. The imaginary part of the index of refraction does not discriminate between absorption and scattering and only contributes to an extinction of the incident wave, according to the Beer-Lambert law. Whereas we expect the use of an effective index of refraction to be well suited for off-resonant scattering, where the atomic polarisability is almost real, such an effective field model has severe limitations in the presence of resonant scattering. Similar situations are also encountered in metamaterials, with different mechanisms at the origin of the resonances [27].

Let us now analyze a better known quantity in transport through random media: the diffuse transmission $T_{\rm diff}$ through a disordered sample. In Fig. (2), we show the result for $T_{\rm diff}$ using the two models which seemed to provide similar results for the intensity distribution inside the sample: the incoherent model and our many body simulation. For large optical thickness, the diffuse transmission is described in the incoherent model by a diffusion equation reminiscent of the Drude model for electrons transmitted through a wire. As a result this model predicts for large b_0: $T_{\rm diff} \propto 1/b_0$, dubbed Ohm's law for photons (black spheres in Fig. 2). We note that energy conservation insures that $T_{\rm diff} + R_{\rm diff} + T_{\rm coh} = 1$, where $R_{\rm diff}$ is the diffuse reflection coefficient and $T_{\rm coh}$ the remaining unscattered coherent forward beam. In contrast to the result of the incoherent model, amounting to neglect all interference effects in multiple scattering, our many body solution provides striking different results for $T_{\rm diff}$ (blue squares in Fig. 2). We have normalized the scattered light across the forward boundary of the slab to the total scattered power (which approaches a constant value at large b0) and checked for energy conservation at low optical thickness. The surprising result is that, instead of a decrease, we observe a saturation for $T_{\rm diff}$ for large b_0, as if the "resistance" for photons to cross this sample would vanish. Resonant scattering of light through a large sample thus violates Ohm's law for photons. We note that in addition to this saturation of the diffuse transmission at a non zero value, the many body simulation also predicts a different slope at small b_0. We attribute this feature, which can be assimilated to a reduced effective optical thickness in the many body simulation, to the consequence of a long range dipole blockade [34].

Further insight can be obtained from the emission diagram. As the cold atom sample used in our experimental setup has a spherical symmetry with a radial Gaussian density distribution $n(r) \propto e^{-r^2/(2\sigma_R^2)}$ and a optical thickness of $b_0 = \int n(0,0,z)\sigma_0 dz = 3N/(k\sigma_r)^2$ we compute the emission diagram for this specific geometry in Fig. 3. The incoherent model (black line in Fig. 3), where photons are isotropically scattered after a distance $1/(n(r)\sigma_0)$, yields a smooth intensity profile, with slightly more photons scattered backwards than forward. We note that for this Gaussian sphere, many photons can be scattered at large distance from the center where the optical thickness is small, yielding a less pronounced backward/forward ratio than a slab geometry. The result of the driven timed Dicke model (green line in Fig. 3) includes the pronounced forward emission lobe as expected from the cooperative interference effect of the scattered light. The more rigorous result of the many body solution (blue line in Fig. 3) in addition includes CBS. This

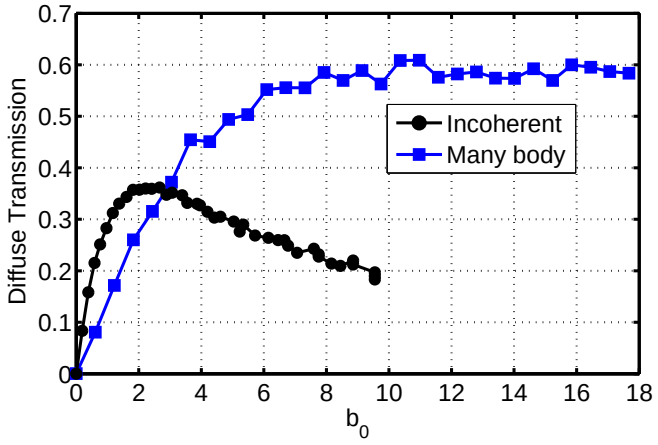

FIG. 2: (color online). Ohm's law for photons. Diffuse transmission of a plane wave through a slab of increasing optical thickness b_0, for the incoherent model (black spheres) and the many body solution (blue squares).

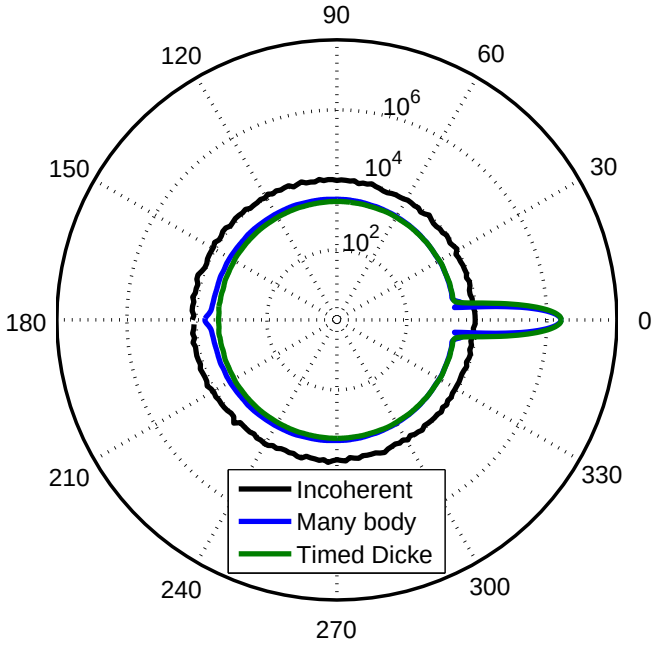

FIG. 3: (color online). Emission diagram obtained numerically for a Gaussian sphere ($k\sigma_R = 20$) of central optical thickness $b_0 = 10$ for the incoherent model using 13000 photons (black line), the timed Dicke Ansatz (green line) and the many body simulation (blue line), averaged over 200 configurations. Logarithmic scale is used for the intensity.

feature, observed in experiments more than 10 years ago [35, 36] is not described by the driven timed Dicke model. Indeed CBS requires dipoles to be excited by the field scattered by others dipoles and not by the incident field alone. In contrast, diagrammatic models which describe CBS by atomic scatterers [37] do not include the physics of superradiance. SFS is thus beyond the reach of such models used in the past to describe resonant multiple scattering.

Possible experimental signatures of SFS obviously include the large diffuse transmission around forward direction. Even though enhanced scattering around backward direction (CBS) has been observed in experiments by direct detection of the scattered light, the direct detection of SFS around forward direction is more challening. Indeed, despite that fact that SFS can be many orders of magnitude larger than CBS, stray scattering by imperfections in experiments often makes direct light detection around forward direction more difficult. We therefore chose to explore a different signature of SFS, exploiting the potential of cold atoms to be an efficient detector of light scattering [20]. As one can anticipate from Fig. 3, incoherent scattering would increase the average radiation pressure force, as more photons are scattered in backward direction. SFS on the contrary leads to a drastic reduction of the radiation pressure force at resonance, as many photons are scattered around the forward direction. We note that CBS also contributes to a modification of the average radiation pressure force (slightly increasing the force), but the amount of light scattered in the CBS cone is so small that its detection via a change of the radiation pressure would be a tour de force.

We thus apply the following experimental procedure to probe SFS in cold atoms. First, we load a magneto-optical trap (MOT) with 3×10^7 atoms of ^{87}Rb in 50 ms using the setup described in [20]. We then apply a 50 ms temporal dark MOT period where the intensity of the repumping laser is reduced by a factor of 10 and the cooling laser is tuned to $-10\,\Gamma$ from the $F = 2 \rightarrow F' = 3$ D_2 line. This allows to compress the cloud and to produce a smooth Gaussian shaped distribution of atoms. To control the optical thickness at the end of this dark MOT period, the repumper detuning is varied between $-7\,\Gamma$ to $-2.5\,\Gamma$, keeping the desired amount of atoms in the $F = 2$ state without affecting the size ($\sigma_R = 270\,\mu$m, $k\sigma_R \approx 2 \times 10^3$), shape and temperature ($\sim 20\,\mu$K) of the cloud. We then switch off all laser beams and magnetic field gradients, leaving the atoms in free fall. We then apply an horizontal, circularly-polarized "pushing" beam, tuned close to the $F = 2 \rightarrow F' = 3$ transition for $50\,\mu$s. The pushing beam has a waist $w_0 = 12$ mm and its carefully calibrated intensity is adjusted to have a saturation parameter $s = 10^{-2}$. Each atom in the $F = 2$ state scatters on average 10 photons. Such a small number of scattered photons prevents from any depumping effect into the $F = 1$ state during the pushing process. After a time of flight expansion of 12 ms, we image the position of the atomic cloud via standard off resonant (detuning $\Delta \approx -2\,\Gamma$) absorption scheme. A Gaussian fit of the absorption image yields the position of the center of mass of the atomic cloud after time of flight and thus the average radiation pressure force. Each experimental

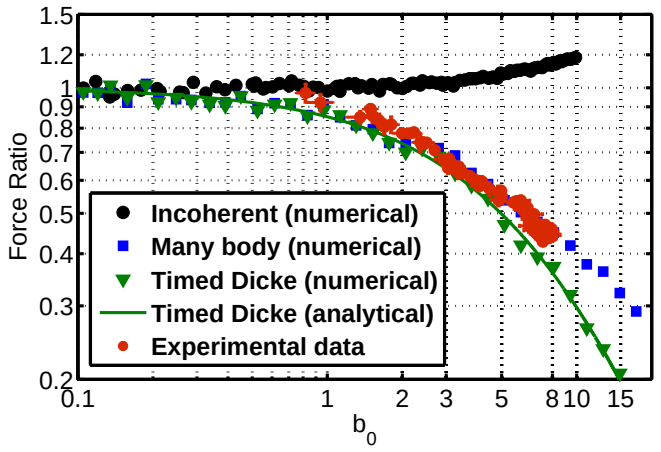

FIG. 4: (color online). Force ratio as the function of optical density b_0 (log-log scale) for resonant laser light.

point (see figure 4) is an average over 10 realizations with error-bars reflecting the shot to shot fluctuations of the experiment. We normalize the measured average radiation pressure force by the single atom force F_1, where F_1 is computed without any adjustable parameter from the measured intensity of the pushing which (known within 5 % accuracy and taking into account losses by the vacuum windows). The experimental value of the optical thickness b_0 is obtained by standard absorption imaging.

In Fig. 4 we show the signature of SFS on the average radiation pressure force. As shown by the numerical results of our many body solution (blue squares), the net result of SFS on the average radiation pressure is a strong reduction of the force. Indeed, as most photons are crossing the sample close to forward direction, the photons leave the system without important transfer of momentum. The larger b_0, the more photons are scattering in the forward lobe of width $\Delta\theta \approx 1/(k\sigma_R)$. The experimental signature of our study of SFS (red spheres with statistical errors bars) clearly shows an important reduction of the average radiation pressure force. This is in striking contrast to the prediction of the incoherent model (black spheres). Indeed, if one could neglect all interference effects for the propagation of light through this optically thick sample of atoms, more and more photons would be scattered backward. For very large b_0, almost no photon would cross the sample (bare a few on the edges of the sample) and the average radiation pressure force would be above that of the independent atom limit. We also indicate on Fig. 4 the prediction using our driven timed Dicke model. We stress that despite the apparent agreement with the experimental values, we do not consider this model to provide an accurate account of the detailed mechanism at work for SFS. Indeed, as shown in Fig. 1, this mean field result does not describe correctly the intensity distribution inside the sample.

We note that despite the agreement between the experimental results and the many body solution, one needs to keep in mind that small systematic corrections could be expected for the calibration of our values of b_0. Indeed we have used a standard low intensity absorption technique to measure b_0. This does not take into account the differences between the transition strengths for various Zeeman sublevels, which could be taken care of by more high intensity absorption imaging [38]. Also, as discussed above, our many body solution is an approximate scalar model. Even if we expect this to capture the main features, in particular for dilute cloud of atoms where near field effects can be neglected, the emission diagram will have some polarization dependence not taken into account by any of the models presented in this work. Minor additional effects which could affect SFS is reduced spatial or temporal coherence as e.g. induced by finite additional disorder, temperature or saturation [24].

In summary, we have introduced an interference effect in multiple scattering based on superradiance. In SFS, Ohm's law for photons is violated and most photons are transmitted through the sample, as if cooperativity would turn a diffuse medium (with a resistance for the transmission of photons) into a superconductor of light. We speculate that similar resonant effects could be induced with different type of resonances (internal resonances, shape resonances or confinement-induced resonances) and applied to different waves (ultra-cold atoms, electrons). We also note that the long range dipole-dipole coupling used in our many body simulations bears some resemblance with the Heisenberg model used at the basis of the resonating valence bond theory [39] and that light scattering by cold atoms might provide a useful toy-model to further study these effects.

Funding from IRSES project COSCALI and from USP/COFECUB is acknowledged. R.B. acknowledges support from the Fundação de Amparo Pesquisa do Estado de São Paulo (FAPESP).

[1] M. P. van Albada, A. Lagendijk, Phys. Rev. Lett. **55**, 2692 (1985).
[2] P.-E. Wolf ,G. Maret, Phys. Rev. Lett. **55**, 2696, (1985).
[3] F. Scheffold, G. Maret, Phys. Rev. Lett. **81**, 5800 (1998).
[4] P. V. Ruijgrok, R. Wuest, A. A. Rebane, A. Renn, and V. Sandoghdar, Opt. Express **18**, 6360 (2010).
[5] M. D. Birowosuto, S. E. Skipetrov, W. L. Vos, and A. P. Mosk, Phys. Rev. Lett. **105**, 013904 (2010).
[6] V. Krachmalnicoff, E. Castanié, Y. De Wilde, and R. Carminati, Phys. Rev. Lett. **105**, 183901 (2010).
[7] D. S. Wiersma, P. Bartolini, A. Lagendijk, and R. Righini, Nature (London) **390**, 671 (1997); D. S. Wiersma, P. Bartolini, A. Lagendijk, and R. Righini, Nature (London) **398**, 206 (1999); F. Scheffold, R. Lenke, R. Tweer, and G. Maret, Nature (London) **398**, 207 (1999).
[8] C. M. Aegerter, M. Storzer and G. Maret, Europhys. Lett. **75**, 562 (2006).

[9] B. A. van Tiggelen, A. Lagendijk, and A. Tip, J. Phys.: Condens. Matter **2**, 7677 (1990).

[10] S. S. Kondov, W. R. McGehee, J. J. Zirbel, B. DeMarco, Science **333**, 66 (2011).

[11] F. Jendrzejewski, A. Bernard, K. Muller, P. Cheinet, V. Josse, M. Piraud, L. Pezze, L. Sanchez-Palencia, A. Aspect, P. Bouyer, Nature Physics **8**, 392 (2012).

[12] G. Labeyrie, T. Karpiuk, J. F. Schaff, B. Gremaud, C. Miniatura, D. Delande, arXiv:1206.0845 (2012).

[13] F. Jendrzejewski, K. Muller, J. Richard, A. Date, T. Plisson, P. Bouyer, A. Aspect, V. Josse, arXiv:1209.1477, to appear in Phys. Rev. Lett. (2012).

[14] A. Tourin, A. Derode, P. Roux, B.A. van Tiggelen, and M. Fink, Phys. Rev. Lett. Phys. Rev. Lett. **79**, 3637 (1997).

[15] H. Hu, A. Strybulevych, J. H. Page, S. E. Skipetrov, B. A. van Tiggelen, Nature Physics **4**, 945 (2008).

[16] R. H. Dicke, Phys. Rev. **93**, 99 (1954).

[17] R. Friedberg, S. R. Hartman, and J. T. Manassah, Phys. Rep. **7**, 101 (1973).

[18] M. O. Scully, E. S. Fry, C. H. R. Ooi, and K. Wodkiewicz, Phys. Rev. Lett. **96**, 010501 (2006).

[19] S. Prasad, R. J. Glauber, Phys. Rev. A **82**, 063805 (2010).

[20] T. Bienaimé, S. Bux, E. Lucioni, P. W. Courteille, N. Piovella, and R. Kaiser, Phys. Rev. Lett. **104**, 183602 (2010).

[21] R. Roehlsberger, K. Schlage, B. Sahoo, S. Couet, and R. Rüffer, Science **328**, 1248-1251 (2010).

[22] J. G. Bohnet, Z. Chen, J. M. Weiner, D. Meiser, M. J. Holland, J. K. Thompson, Nature **484**, 78 (2012).

[23] E. Akkermans, A. Gero, R. Kaiser, Phys. Rev. Lett. **101**, 103602 (2008).

[24] T. Bienaimé, N. Piovella, and R. Kaiser, Phys. Rev. Lett. **108**, 123602 (2012).

[25] K. Busch, C. M. Soukoulis, Phys. Rev. Lett. **75**, 3442 (1995).

[26] D. Vollhardt and P. Wolfle, Phys. Rev. Lett. **45**, 842 (1980).

[27] V.A. Markel, J. C. Schotland, Phys. Rev. E **85**, 066603 (2012).

[28] T. Lee, K. Huang, and C. Yang, Phys. Rev. **106**, 1135 (1957).

[29] N. Navon, S. Piatecki, K. Gunter, B. Rem, T. C. Nguyen, F. Chevy, W. Krauth, and C. Salomon, Phys. Rev. Lett. **107**, 135301 (2011).

[30] T. Bienaimé, M. Petruzzo,D. Bigerni, N. Piovella and R. Kaiser, J. Mod. Opt. **58**, 1942 (2011).

[31] Ph. W. Courteille, S. Bux, E. Lucioni, K. Lauber, T. Bienaimé, R. Kaiser, N. Piovella, Eur. Phys. J. D, **58**, 69 (2010).

[32] R. Bachelard, Ph. Courteille, R. Kaiser, N. Piovella, Europhys. Lett. **97**, 14004 (2012).

[33] J. T. Manassah, Advances in Optics and Photonics **4**, 108 (2012).

[34] T. Bienaimé, R. Bachelard, N. Piovella, and R. Kaiser, arXiv:1204.5598, to appear in Fortschr. Phys. (2012).

[35] G. Labeyrie, F. de Tomasi, J.-C. Bernard, C. A. Müller, Ch. Miniatura and R. Kaiser, Phys. Rev. Lett., **83**, 5266 (1999).

[36] P. Kulatunga, C. I. Sukenik, S. Balik, M. D. Havey, D. V. Kupriyanov and I. M. Sokolov, Phys. Rev. A **68**, 033816 (2003).

[37] T. Jonckheere, C. A. Müller, R. Kaiser, Ch. Miniatura and D. Delande, Phys. Rev. Lett. **85**, 4269 (2000).

[38] G. Reinaudi, T. Lahaye, Z. Wang, and D. Guéry-Odelin, Opt. Lett. **32**, 3143 (2007).

[39] P. W. Anderson, Science, **235**, 1196 (1987).